Transmembrane Proteins

DOI: 10.1002/ange.201408707

Cell-Derived Vesicles for Single-Molecule Imaging of Membrane Proteins**

*Faruk H. Moonschi, Amy K. Effinger, Xiaolu Zhang, William E. Martin, Ashley M. Fox, David K. Heidary, Jason E. DeRouchey, and Christopher I. Richards**

Abstract: *A new approach is presented for the application of single-molecule imaging to membrane receptors through the use of vesicles derived from cells expressing fluorescently labeled receptors. During the isolation of vesicles, receptors remain embedded in the membrane of the resultant vesicles, thus allowing these vesicles to serve as nanocontainers for single-molecule measurements. Cell-derived vesicles maintain the structural integrity of transmembrane receptors by keeping them in their physiological membrane. It was demonstrated that receptors isolated in these vesicles can be studied with solution-based fluorescence correlation spectroscopy (FCS) and can be isolated on a solid substrate for single-molecule studies. This technique was applied to determine the stoichiometry of α3β4 nicotinic receptors. The method provides the capability to extend single-molecule studies to previously inaccessible classes of receptors.*

Complex protein structures, such as membrane receptors, regulate many aspects of cellular function, including the initiation of signal transduction pathways.[1] Transient interactions between proteins often complicate efforts to fully understand the function of specific biomolecules.[2] The primary challenge is that a single species can exist in multiple conformational or functional states. Single-molecule approaches are often employed to resolve these dynamics since they avoid ensemble averaging across multiple states, but the physiological concentration of receptors is often too high for single-molecule measurements. Furthermore, isolating individual proteins poses a challenge for receptors since they tend to aggregate on the cell surface. A common approach to overcome this concentration barrier[3] is to isolate biomolecules from the cell.[4] This approach only works for proteins that can either be solubilized or stabilized in a detergent solution. As a result, a variety of approaches have been employed to isolate receptors or to apply single-molecule techniques in cells.[3,5,6] For example, sub-micron liposomal vesicles composed of artificial bilayers have been utilized as nanocontainers for the isolation of proteins.[7] This approach requires receptors to be temporarily supported in a detergent solution. This presents a major disadvantage in that receptors are completely removed from their physiological environment.

Herein, we introduce a single-molecule approach in which receptors are isolated in vesicles generated from cell membranes. Microsomes and other cell-derived vesicles are widely used for biochemical applications to study membrane receptors and other proteins.[8] We utilized a similar strategy by generating vesicles from cells expressing a protein of interest in order to perform single-molecule imaging. This approach leaves membrane proteins embedded in the same physiological membrane in which they resided within the cell. The use of these vesicles eliminates the need to support proteins in a detergent environment or to encapsulate them in vesicles composed of artificial membranes. We demonstrated the versatility of this method by using several classes of membrane receptors, and we expanded this technique to determine the stoichiometry of multisubunit α3β4 nicotinic receptors.

Procedures for the separation of vesicles from cell lysates have become standard for biochemical applications.[9] In our studies, vesicles were generated from cells transfected with fluorescently labeled receptors (Figure 1). During translation, receptor subunits are directly inserted into the membrane of the endoplasmic reticulum (ER). For oligomeric protein structures, these subunits are rapidly assembled into receptors and queued for transport to the plasma membrane (PM).[10] In order to isolate single receptors expressed in these cell membranes, we fragmented cells by using nitrogen cavitation with a pressure of approximately 250 psi for 5 min to form membrane vesicles (see the Supporting Information).[11] The resulting individual membrane fragments spontaneously reform to create vesicles. Vesicles were separated from the cell lysate through differential ultracentrifugation. Any receptors supported in the membrane fragments are confined in the lipid bilayer of the resulting vesicles. We incorporated fluorescent labels and epitope binding sites into the receptors to facilitate the immobilization of the vesicles on a substrate (Figure 1).

The homogenization of cells has been shown to generate vesicles ranging in size from 100 to 300 nm in diameter.[12] In order to determine the size of the vesicles in our preparations, we transfected HEK293T cells with α3-GFP and β4-GFP nicotinic receptor subunits. Diffusion times in fluorescence correlation spectroscopy (FCS) measurements were employed to determine the size of the vesicles, which were found to have a mean diameter of 180 ± 20 nm (Figure S1 in the Supporting Information). To determine whether vesicles

[*] F. H. Moonschi, A. K. Effinger, X. Zhang, W. E. Martin, A. M. Fox, Dr. D. K. Heidary, Prof. J. E. DeRouchey, Prof. C. I. Richards
Department of Chemistry, University of Kentucky
505 Rose Street, Lexington, KY 40506 (USA)
E-mail: chris.richards@uky.edu

[**] We thank L. B. Hersh for a gift of HEK cells, A. Sorkin for EGFR-GFP (Addgene plasmid 32751), and E. Glazer for technical support. Support from (KSEF-2819-RDE-016).

Supporting information for this article is available on the WWW under http://dx.doi.org/10.1002/anie.201408707.

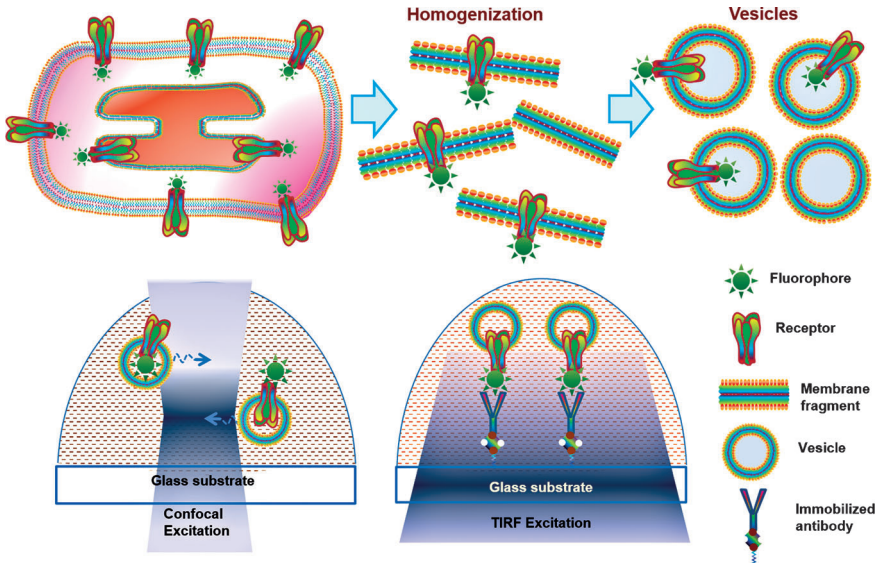

Figure 1. Single-molecule imaging in vesicles composed of cell membranes. Cells are homogenized to generate membrane fragments, which reorganize to form vesicles. Receptors are encapsulated in the vesicle membrane. The resulting cell-derived vesicles can be used to study receptors in solution or immobilized on a substrate.

of this size can be used to isolate single receptors, we expressed the epidermal growth factor receptor (EGFR) or cystic fibrosis transmembrane regulator (CFTR) in HEK293T cells. CFTR is a large (ca. 170 kDa) membrane chloride channel that is difficult to isolate from cells and can only be purified in small quantities. We generated vesicles from cells expressing either CFTR or EGFR and immobilized them on glass substrates. By using total internal reflection fluorescence (TIRF) microscopy, we determined the number of receptors per vesicle by counting GFP photobleaching steps during continuous excitation (Figure S2).[6,13] We were able to generate receptors with single-step bleaching, which is indicative of the presence of a monomer for both types of receptors (Figures S2 and S3).

Heteromeric nicotinic receptors assemble as pentamers composed of two or more different types of subunits. Some subtypes have been reported to assemble with multiple stoichiometries,[6] but little is known about the assembly of α3β4 nicotinic receptors. We transfected HEK293T or mouse neuroblastoma (N2a) cells with plasmids encoding GFP-tagged mouse α3 (α3-GFP) and wildtype β4 (β4-wt), or α3-wt and β4-GFP nicotinic receptor subunits. These constructs have been used extensively in the past and the incorporation of the fluorescent protein does not affect the function of the receptor.[14] A TIRF image of an N2a cell expressing α3-GFP and β4-wt is shown in Figure 2A. We next generated vesicles from these cells and examined the fluorescence in solution. The steady-state emission spectrum (Figure 2B) matches that of GFP. Once immobilized on the surface of a glass substrate, TIRF microscopy revealed that vesicles containing α3-GFP/β4-wt or α3-wt/β4-GFP receptors were well dispersed across the surface (Figure 2C). By using an electron multiplying charge-coupled device (CCD), we recorded time versus intensity measurements for multiple vesicles and then determined the number of labeled subunits per vesicle by counting single-molecule photobleaching steps.[15] The number of bleaching levels corresponds to the number of subunits. Representative time traces of single vesicles showing two- and three-step bleaching are shown in Figure 3A and Figure 3C, respectively. We plotted the distribution of the number of bleaching steps when the α subunit was labeled and separately when the β subunit was labeled and compared these to binomial distributions to account for the possibility of two stoichiometries (see the Supporting Information). Binomial distributions weighted for 2(α3):3(β4) 75% of the time and 3(α3):2(β4) 25% of the time fit well with the observed distributions for both α3-GFP/β4-wt and α3-wt/β4-GFP data sets (Figure 3). The distribution of bleaching steps shows that α3β4 has a primary stoichiometry of 3:2 (75%) and a minor stoichiometry of 2:3 (25%). The full distribution of observed steps is shown in Table S1 in the Supporting Information.

We also performed two-color single-molecule measurements on nicotinic receptors by using α3 conjugated to mCherry, a red fluorescent protein, with β4-GFP. This allowed us to perform measurements to simultaneously identify all 5 subunits within a receptor. We then performed photobleaching step analysis with sequential 561 nm and 488 nm excitation. Figure 4 shows representative images of the same field of view excited at 561 nm (panel A) or 488 nm (panel B), and an overlay of the images (panel C). Clear overlap is seen between the two images for the majority of punctate regions. For those vesicles showing overlap, we examined the time traces for both channels, counting the bleaching steps for each. Time traces from the mCherry channel (Figure 4D) and the GFP channel (Figure 4E) for the same vesicle were used to determine the stoichiometry.

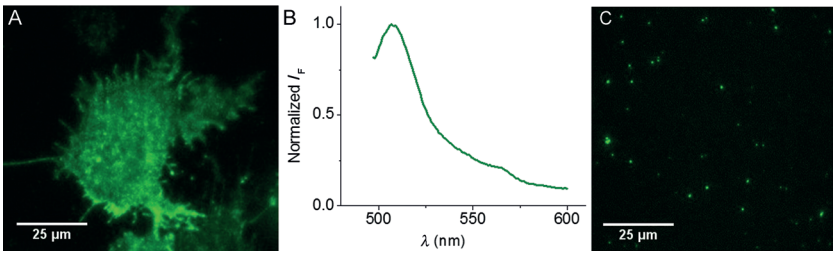

Figure 2. A) TIRF image of an N2a cell expressing α3-GFP/β4-wt. B) Steady-state fluorescence of a solution containing vesicles isolated from cells expressing α3-GFP/β4-wt. C) TIRF image of isolated vesicles containing α3-GFP/β4-wt.

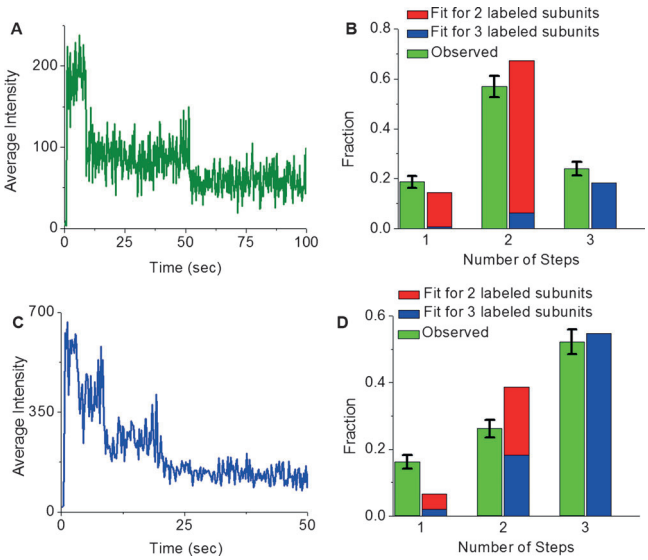

Figure 3. Determination of the stoichiometry of α3β4 nicotinic receptors. A) Time trace for a vesicle containing α3-GFP/β4-wt receptors showing two bleaching steps. B) The observed and fitted [75% 2(α3):3(β4) and 25% 3(α3):2(β4)] distributions of one, two, and three bleaching steps for α3-GFP/β4-wt. C) Time trace for a vesicle expressing α3-wt/β4-GFP, showing three bleaching steps. D) The observed and fitted [75% 2(α3):3(β4) and 25% 3(α3):2(β4)] distributions of one, two, and three bleaching steps for α3-wt/β4-GFP.

Figure 4, panels D and E show two bleaching steps for mCherry and three bleaching steps for GFP, respectively. Restricting accepted spots to those containing five measured subunits provided a direct readout of the stoichiometry (see the Supporting Information). These studies show a stoichiometry of 80% 2:3 (α3:β4) and 20% 3:2 (α3:β4), as shown in Figure 4F. This is similar to the stoichiometry determined by using GFP alone.

To verify that the nicotinic receptors isolated in vesicles maintain functionality, we performed Ca^{2+} flux studies.[16] A glass substrate functionalized with an anti-flag antibody was used to immobilize vesicles containing α7-GFP and β2-Flag (see the Supporting Information). Prior to immobilization, the vesicles were loaded with Fluo-8 AM, a Ca^{2+} sensitive fluorophore.[16] Upon immobilization, vesicles were located by visualizing the GFP fluorescence (Figure S4), and the GFP signal was then bleached. A buffer containing Ca^{2+} and acetylcholine (ACh) was added to activate receptors. Ca^{2+} induced Fluo-8 fluorescence was then used to identify vesicles containing functional receptors. Approximately 60% of the vesicles exhibiting GFP fluorescence showed functional activity.

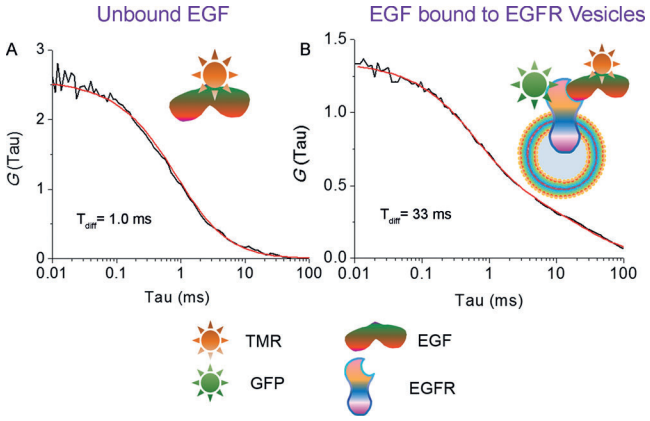

Figure 5. Ligand binding to receptors embedded in vesicles. A) Autocorrelation curve for free EGF-TMR, showing a diffusion time of ca. 1 ms. B) Autocorrelation curve for EGF-TMR mixed with EGFR vesicles, showing a diffusion time of 33 ms. Black: data, red: fit.

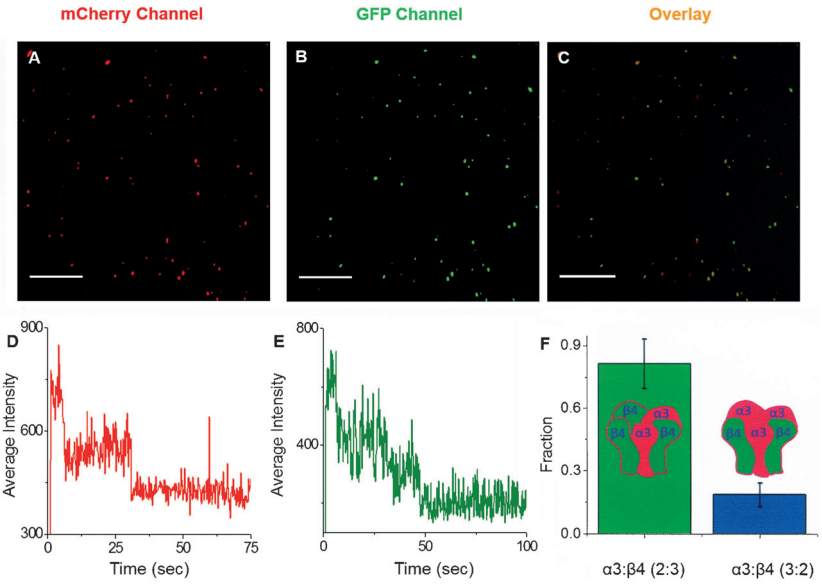

Figure 4. Simultaneous multicolor bleaching step analysis in vesicles. TIRF image of vesicles with α3-mCherry fluorescence (A), β4-GFP fluorescence (B), and an overlay (C) are shown. Representative bleaching steps are shown for mCherry (D) and GFP (E). F) Distribution of vesicles showing a 2(α3):3(β4) stoichiometry. Error bars: 25 μm

To demonstrate that receptors isolated in vesicles can be used for binding studies,[17] we generated vesicles containing EGFR-GFP. These vesicles exhibit a diffusion time of approximately 33 ms. Similar measurements (561 nm excitation) of fluorescently labeled epidermal growth factor (EGF) conjugated to tetramethylrhodamine (TMR) exhibited a diffusion time of approximately 1 ms (Figure 5A). The binding of EGF to EGFR has been demonstrated under many conditions.[18] A clear increase in the diffusion time (1 ms to 33 ms) was observed for EGF-TMR combined with vesicles containing EGFR-GFP. The shift in diffusion time reflects the binding of EGF to EGFR-containing vesicles (Figure 5B). Similar control experiments with nicotinic receptor vesicles did not show this shift (Figure S10).

We have demonstrated that cell-derived vesicles can be utilized for single-molecule

studies of receptors. This approach allows receptors to be maintained in their native cellular membrane. To demonstrate the versatility of this approach, we performed single-molecule measurements on both immobilized receptors and those in solution. Furthermore, we were able to determine that α3β4 nicotinic receptors preferentially form a 2:3 stoichiometry. This approach allowed us to overcome the concentration barrier inherent to single-molecule studies in cells that results from high protein expression levels. With this method, single-molecule experiments can be extended to new classes of membrane receptors that are not typically accessible to single-molecule measurements.

Received: September 1, 2014
Revised: October 1, 2014
Published online: October 31, 2014

Keywords: fluorescence correlation spectroscopy · fluorescence microscopy · transmembrane proteins · single-molecule studies · vesicles

[1] D. Mowrey, Q. Chen, Y. Liang, J. Liang, Y. Xu, P. Tang, *PLoS One* **2013**, *8*, e64326; J. J. Lacroix, F. V. Campos, L. Frezza, F. Bezanilla, *Neuron* **2013**, *79*, 651 – 657.

[2] S. R. Grady, R. M. Drenan, S. R. Breining, D. Yohannes, C. R. Wageman, N. B. Fedorov, S. McKinney, P. Whiteaker, M. Bencherif, H. A. Lester, M. J. Marks, *Neuropharmacology* **2010**, *58*, 1054 – 1066.

[3] P. Holzmeister, G. P. Acuna, D. Grohmann, P. Tinnefeld, *Chem. Soc. Rev.* **2014**, *43*, 1014 – 1028; A. B. Loveland, S. Habuchi, J. C. Walter, A. M. van Oijen, *Nat. Methods* **2012**, *9*, 987 – 992.

[4] A. Jain, R. Liu, B. Ramani, E. Arauz, Y. Ishitsuka, K. Ragunathan, J. Park, J. Chen, Y. K. Xiang, T. Ha, *Nature* **2011**, *473*, 484 – 488; H. S. Chung, K. McHale, J. M. Louis, W. A. Eaton, *Science* **2012**, *335*, 981 – 984.

[5] S. Uemura, C. E. Aitken, J. Korlach, B. A. Flusberg, S. W. Turner, J. D. Puglisi, *Nature* **2010**, *464*, 1012-U1073.

[6] C. I. Richards, K. Luong, R. Srinivasan, S. W. Turner, D. A. Dougherty, J. Korlach, H. A. Lester, *Nano Lett.* **2012**, *12*, 3690 – 3694.

[7] B. Liu, A. Mazouchi, C. C. Gradinaru, *J. Phys. Chem. B* **2010**, *114*, 15191 – 15198.

[8] L. Pronsato, R. Boland, L. Milanesi, *Arch. Biochem. Biophys.* **2013**, *530*, 13 – 22; E. Kaznacheyeva, V. D. Lupu, I. Bezprozvanny, *J. Gen. Physiol.* **1998**, *111*, 847 – 856.

[9] Y. Li, M. Ge, L. Ciani, G. Kuriakose, E. J. Westover, M. Dura, D. F. Covey, J. H. Freed, F. R. Maxfield, J. Lytton, I. Tabas, *J. Biol. Chem.* **2004**, *279*, 37030 – 37039.

[10] F. Mazzo, F. Pistillo, G. Grazioso, F. Clementi, N. Borgese, C. Gotti, S. F. Colombo, *J. Neurosci.* **2013**, *33*, 12316 – 12328.

[11] R. M. Dowben, P. M. Lynch, H. L. Nadler, D. Y. Hsia, *Exp. Cell Res.* **1969**, *58*, 167 – 169.

[12] K. Kawajiri, A. Ito, T. Omura, *J. Biochem.* **1977**, *81*, 779 – 789; M. Wibo, A. Amar-Costesec, J. Berthet, H. Beaufay, *J. Cell. Biol.* **1971**, *51*, 52 – 71.

[13] P. Hastie, M. H. Ulbrich, H. L. Wang, R. J. Arant, A. G. Lau, Z. Zhang, E. Y. Isacoff, L. Chen, *Proc. Natl. Acad. Sci. USA* **2013**, *110*, 5163 – 5168.

[14] B. J. Henderson, R. Srinivasan, W. A. Nichols, C. N. Dilworth, D. F. Gutierrez, E. D. Mackey, S. McKinney, R. M. Drenan, C. I. Richards, H. A. Lester, *J. Gen. Physiol.* **2013**, *143*, 51 – 66; R. Srinivasan, C. I. Richards, C. Dilworth, F. J. Moss, D. A. Dougherty, H. A. Lester, *Int. J. Mol. Sci.* **2012**, *13*, 10022 – 10040.

[15] M. H. Ulbrich, E. Y. Isacoff, *Nat. Methods* **2007**, *4*, 319 – 321.

[16] T. L. Smith, *Neurochem. Int.* **1990**, *16*, 89 – 94; S. Vernino, M. Rogers, K. Radcliffe, J. Dani, *J. Neurosci.* **1994**, *14*, 5514 – 5524.

[17] A. C. Ferreon, Y. Gambin, E. A. Lemke, A. A. Deniz, *Proc. Natl. Acad. Sci. USA* **2009**, *106*, 5645 – 5650; S. Elbaum-Garfinkle, G. Cobb, J. T. Compton, X. H. Li, E. Rhoades, *Proc. Natl. Acad. Sci. USA* **2014**, *111*, 6311 – 6316.

[18] E. Luković, E. V. Taylor, B. Imperiali, *Angew. Chem. Int. Ed.* **2009**, *48*, 6828 – 6831; *Angew. Chem.* **2009**, *121*, 6960 – 6963.

